DALTON
FULL PAPER

Synthesis and characterization of the tetraazamacrocycle 4,10-dimethyl-1,4,7,10-tetraazacyclododecane-1,7-diacetic acid (H_2Me_2DO2A) and of its neutral copper(II) complex [$Cu(Me_2DO2A)$]. A new ^{64}Cu-labeled macrocyclic complex for positron emission tomography imaging †

Pierluigi Barbaro,[a] Claudio Bianchini,*[a] Geraldo Capannesi,[b] Lorella Di Luca,[d] Franco Laschi,[c] Debora Petroni,[d] Piero A. Salvadori,[d] Alberto Vacca[e] and Francesco Vizza*[a]

[a] *ISSECC-CNR, Via J. Nardi 39, Firenze-50132, Italy*
[b] *ENEA-Casaccia, Rome-00060, Italy*
[c] *Università di Siena, via AldoMoro 1, Siena-53100, Italy*
[d] *CNR-IFC, via P. Salvi 8, Pisa-56100, Italy*
[e] *Università di Firenze, via Maragliano 77, Firenze-50144, Italy*

Received 28th March 2000, Accepted 31st May 2000
Published on the Web 30th June 2000

The new macrocycle 4,10-dimethyl-1,4,7,10-tetraazacyclododecane-1,7-diacetic acid (H_2Me_2DO2A, H_2L) has been synthesized and characterized. The basicity constants of the macrocycle and the stability constants of its complex formation with copper(II) ions have been determined in aqueous solution by potentiometry. The protonation sequence of the macrocycle has been studied by ^{1}H and ^{13}C-{^{1}H} NMR spectroscopy. The data obtained are consistent with the first and second protonations taking place at the methyl-substituted nitrogen atoms, while the third and fourth protonations involve the two carboxylate arms. High-resolution NMR studies have revealed that the ethylenic protons in the tetraprotonated H_4L^{2+} species are inequivalent due to multiple hydrogen bonds within the macrocycle ring, indicating that the system is locked in a rigid conformation on the NMR timescale. The molecular structure of the copper(II) complex [$Cu(Me_2DO2A)$]·$2H_2O$ has been determined by a single crystal X-ray analysis. The macrocycle wraps the metal in a distorted octahedral geometry using the four nitrogen atoms and two oxygen atoms from the two carboxylate groups. These latter are *cis* to each other. The excellent stability of [$Cu(Me_2DO2A)$] at physiological pH is confirmed by a cyclic voltammetry study that shows the complex to be irreversibly reduced at $E_p = -0.81$ V. The radioactive ^{64}Cu-labeled complex [$^{64}Cu(Me_2DO2A)$] has been synthesized using $^{64}CuCl_2$. Animal biodistribution studies have been performed by bolus injection in rabbit and followed by Positron Emission Tomography (PET), an *in vivo* imaging technique used in nuclear medicine to detect the regional distribution and concentration of positron emitting radionuclides. PET images showed that the tested compound has high uptake in liver, kidneys and bladder. A significant uptake of radioactivity is observed in brain.

Introduction

Paramagnetic and/or radioactive metal complexes stabilized by polyazamacrocycles with dangling ligating groups[1] are receiving increasing attention for their considerable potential in diagnostic[2] and therapeutic medicine.[3] The preference for this kind of polyazamacrocyclic complex over other ligand–metal systems is motivated by some favorable features: ease of synthesis, relatively small size, excellent kinetic and thermodynamic stability of the resulting metal complexes which are generally soluble in water and exhibit remarkable resistance to metal ion exchange *in vivo*.[4] In addition, polyazamacrocyclic systems have the further advantage of being easily tuned and tailored so as to address specific issues regarding the dimensions of both the metal ion and the chelating cavity of the macrocycle, the relative positions of the donor atoms within the macrocyclic ring, the electronic and steric nature of the peripheral ligands. These comprise various anionic[5] and neutral[6] groups with different donor atoms and thus may determine the overall charge of the metal complexes.

Among the various radioisotopes suitable for clinical application in nuclear medicine, copper radionuclides exhibit a number of interesting features.[7] Indeed, ^{64}Cu is a versatile radionuclide which exhibits both electron capture decay (41%) with associated Auger electron emission ($E = 6.5$–0.8 keV) and β^- (40%, $E = 190$ keV) and β^+ (19%, $E = 278$ keV) nuclear decays. The half-life time of ^{64}Cu (12.7 h) is long enough to allow for the synthesis of many radiopharmaceutical compounds and is compatible with *in vivo* kinetics of many biochemical processes. Interestingly, β^+ emission makes ^{64}Cu suitable for application in Positron Emission Tomography (PET), an important imaging diagnostic technique which is currently used for the assessment of *in vivo* biological processes, while β^- particle emission and Auger electrons makes this radionuclide applicable to metabolic radiotherapy.

In general, copper(II) complexes with nitrogen ligands show excellent blood stability *in vivo*.[8–10] Some examples of polyazamacrocycle complexes of ^{62}Cu, $^{64}Cu^{II}$ and $^{67}Cu^{II}$ conjugated to human serum albumin have been used for blood pool imaging[11] and used in biomedical application as bifunctional agents, *e.g.* bound to monoclonal antibodies.[12–21]

Relevant studies have recently been reported by Anderson and co-workers[22] on the biodistribution of some azamacrocycle complexes of ^{64}Cu in Dawley rats. These authors have clearly

† Electronic supplementary information (ESI) available: plots of ^{13}C NMR chemical shift *vs.* pH, NOESY, COSY and HMQC spectra. See http://www.rsc.org/suppdata/dt/b0/b002441o/

DOI: 10.1039/b002441o

shown that the biodistribution of ^{64}Cu labeled macrocycles depends on both the macrocycle skeleton and the formal charge of the complex.

The potential of radioactive copper(II) ions/polyazamacrocycle assemblies in diagnostic and therapeutic medicine attracted our attention and prompted us to develop a research project aimed at synthesizing new complexes of $^{64}Cu^{II}$ with functionalized polyazamacrocycles. Our primary strategy was to look at both ^{64}Cu complexes, as they allow for PET monitoring, and neutral polyazamacrocyclic complexes. Indeed, we thought that, by varying the lipophilicity of the complexes, different specificities in their biodistribution would have been obtained and specific biochemical processes would have been induced.

In this paper are described the synthesis and characterization of a new N-functionalized cyclen macrocycle, 4,10-dimethyl-1,4,7,10-tetraazacyclododecane-1,7-diacetic acid) (H_2Me_2-DO2A) and of its copper(II) complex [Cu(Me_2DO2A)] **1**.

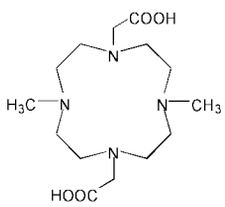

H_2Me_2DO2A

The ^{64}Cu labeled complex was also synthesized and used to carry out PET biodistribution studies following *in vivo* administration to rabbit. Although to a low extent, this complex was found to cross the blood–brain barrier. This is particularly important as brain is an interesting target from the viewpoint of both pathophysiology and physiology and many research efforts are being made to prepare new tracers to study its function. Radiotracer uptake by brain is actually related to the ability of the radionuclide complex to cross the blood–brain barrier as only relatively low-molecular-weight, neutral and lipophilic complexes may cross the membrane. A deep understanding of the *in vivo* biochemistry and clearance properties of the radiometal chelate is hence essential to design specific radiotracers for clinical application.

Experimental

General information

1,7-Dimethyl-1,4,7,10-tetraazacyclododecane was prepared as described in the literature.[23] Deuteriated solvents for NMR measurements (Merck, Aldrich) were dried over molecular sieves. All the other reagents and chemicals were reagent-grade and used as received from commercial suppliers. Infrared spectra were recorded on a Perkin-Elmer 1600 Series FT-IR spectrophotometer using samples mulled in Nujol between KBr plates, ^1H and ^{13}C-{^1H} NMR spectra at 200.13 and 50.32 MHz, respectively (Bruker 200-ACP) or at 500.132 and 125.76 MHz, respectively (Bruker Avance DRX-500). Chemical shifts are relative to tetramethylsilane as external reference or calibrated against solvent resonances. The assignments of the signals resulted from 2-D ^1H COSY, ^1H NOESY and proton detected ^1H–^{13}C correlations using degassed non-spinning samples. 2-D NMR spectra were recorded on a Bruker Avance DRX-500 spectrometer using pulse sequences suitable for phase-sensitive representations using TPPI (time proportional phase incrementation). The ^1H–^{13}C correlations[24] were recorded using an HMQC (heteronuclear multiple quantum correlation) sequence which allows for the measurements of J_{HC} coupling constants. ^1H NOESY[25] spectra were acquired with 1024 increments of size 2K covering the full range in both dimensions with a mixing time of 600 ms.

Solutions of Me_2DO2A (0.03 M) for NMR pH titration were prepared in D_2O and the desired pD was adjusted with standard 1 M solutions of DCl or KOD. The final pD was determined with an Orion Research 601 I Digital Ionalyzer apparatus equipped with a combined glass Ag–AgCl microelectrode (Ingold) which was standardized against standard aqueous buffers at pH 4 and 7. The pD was calculated using the empirical relationship D = "pH meter reading" + 0.40.[26a,b] Although pD values and pH values cannot strictly be compared, it was found that pD values for a number of buffers in D_2O lie about 0.6 logarithmic unit higher than the pH values for the same buffers of the same concentration in H_2O.[26c] This allows a rough correction for the deuterium isotope effect using the relation pH = pD − 0.6.[26c,d] The ^1H and ^{13}C NMR spectra for pH titrations were performed on the Bruker 200-ACP (200.13; 50.32 MHz) instrument at a probe temperature of 25 °C. GC analyses were performed on a Shimadzu GC-14A gas chromatograph equipped with a flame ionization detector and a 30 m (0.25 mm i.d., 0.25 μm film thickness) SPB-1 Supelco fused silica capillary column. GCMS analyses were performed on a Shimadzu QP 5000 apparatus equipped with a column identical to that used for GC analyses. Elemental analyses (C, H, N) were performed using a Carlo Erba Model 1106 elemental analyzer. Conductivities were measured with a Model 990101 Orion Conductance Cell connected to a Model 101 conductivity meter.

Preparations

4,10-Dimethyl-1,4,7,10-tetraazacyclododecane-1,7-diacetic acid–hydrochloric acid–water (1/3/1) ($H_2Me_2DO2A\cdot3HCl\cdot H_2O$). Chloroacetic acid (9.4 g, 0.1 mmol) in water (20 cm^3) was added to a solution of 1,7-dimethyl-1,4,7,10-tetraazacyclododecane (2 g, 0.01 mmol) in water (30 cm^3) and the pH adjusted to 9.0 with 5 M NaOH. The temperature was raised to 70 °C and the pH maintained between 8.5 and 9.0 with addition of 5 M NaOH as necessary. The solution was maintained at this temperature for 15 h, then cooled to room temperature. After the pH was brought to 7 with 5 M HCl, the solution was passed through a cation-exchange column (Amberlite IR 120; H^+ form, bed volume 40 cm^3). The column was washed with water (150 cm^3) until the eluent was neutral and the ligand brought off the column with 300 cm^3 of 0.5 M NH_4OH. The solvent was removed under vacuum to yield the ammonium salt of the ligand. This was dissolved in 100 cm^3 of deionized water and passed through a column of anion-exchange resin (Amberlite IRA 900, in its alkaline form, bed volume 40 cm^3) which was washed with water (250 cm^3) before eluting the ligand with 100 cm^3 of 5 M HCl. The solvent was removed in vacuum to leave a white solid of formula $C_{14}H_{28}N_4O_4\cdot3HCl\cdot H_2O$. Yield 40%. The numbering scheme for the carbon and hydrogen atoms is given in Fig. 2. ^1H NMR (500.132 MHz, D_2O, pH 2.0, 25 °C): δ 2.91 (6 H, s, NMe), 3.52 (4 H, s, H_D), 3.44 (4 H, ddd, H_B, $^2J_{BB'}$ = 14.2, $^3J_{CB}$ = 3.5, $^3J_{C'B}$ = 7.2), 3.24 (4 H, ddd, $H_{B'}$, $^3J_{CB'}$ = 7.5, $^3J_{C'B'}$ = 3.3), 3.09 (4 H, ddd, H_C, $^2J_{CC'}$ = 15.4 Hz) and 2.94 (4 H, ddd, $H_{C'}$). ^{13}C-{^1H} NMR (125.76 MHz, D_2O, pH 2.0, 25 °C): δ 176.10 (C_E), 43.60 (C_A), 54.79 (C_D), 53.86 (C_B) and 49.80 (C_C) (Found: C, 38.2; H, 7.94; N, 13.12%. $C_{14}H_{28}N_4O_4\cdot3HCl\cdot H_2O$ requires C, 38.00; H, 7.52; N, 12.67%).

[Cu(Me_2DO2A)]·3H_2O. CAUTION: perchlorate salts of metal complexes are potentially explosive and must be handled with care. $H_2Me_2DO2A\cdot3HCl\cdot H_2O$ (0.2 g, 0.45 mmol) was dissolved in water (5 cm^3) and the pH adjusted to 7.4 by addition of 10 M NaOH. A solution of $Cu(ClO_4)_2\cdot6H_2O$ (0.166 mmol) in ethanol (10 cm^3) was slowly added at room temperature. The resulting solution was gently heated to 50 °C for 5 min. On addition of ethanol (15 cm^3) and standing at room temperature, blue crystals slowly separated which were filtered off and then recrystallized from 1 : 3 water–ethanol. Yield 70% (Found: C, 39.2; H, 7.58; N, 13.01%. $C_{14}H_{26}CuN_4O_4\cdot3H_2O$ requires C, 38.93; H, 7.47; N, 12.97%); IR ν_{asym}/cm^{-1} 1610 (CO_2^-). Crystals

of $[Cu(Me_2DO2A)]\cdot 3H_2O$, suitable for an X-ray analysis, were obtained by slow recrystallization from a diluted water/EtOH/DMF solution at room temperature.

[^{64}Cu(Me$_2$DO2A)]. No carrier free ^{64}Cu was produced at the TRIGA nuclear reactor of Ente Nazionale Energie Alternative (ENEA)-Casaccia (Rome). Target material was made of ultra pure $CuCl_2\cdot 2H_2O$ and ranged from 25 to 50 mg (corresponding to 10–20 mg of copper); the target blades were quartz and aluminium. Final activity, after 26 hours of neutron bombardment (2.6×10^{13} n^4 cm^{-2} s^{-1} at 220 °C) was 7.5 mCi mg^{-1} (99.99% of radiochemistry purity). To a solution of $Me_2DO2A\cdot 3HCl\cdot H_2O$ (0.01 g, 0.026 mmol) in 1 cm^3 of water was added 150 μL of a solution of $^{64}CuCl_2$ in 0.1 M HCl (0.024 mmol, 500 μCi) at room temperature. The pH was adjusted to 7.4 by addition of 5 M NaOH. The resulting solution changed from light to dark blue indicating formation of the copper complex. This solution was used for biodistribution studies.

Potentiometry

$NaClO_4$ and NMe_4Cl were analytical grade commercial products (Merck), purified by double recrystallization from ethanol–water prior to use. Carbon dioxide-free water was produced from deionized water which was distilled twice in a quartz apparatus and stored under purified nitrogen. An approximately 0.15 M NMe_4OH solution, prepared by dilution of a commercial concentrated solution (Fluka, puriss. p. a.), was stored under nitrogen and its concentration checked before and after each potentiometric experiment by titration against potassium hydrogenphthalate (Fluka, puriss. p. a.). A 0.1 M stock solution of copper chloride was prepared by dissolving analytical grade $CuCl_2\cdot 2H_2O$ (Merck) in water and the copper content determined gravimetrically as salicylaldoximate. emf titrations were carried out using a Crison Micro pH 2002 potentiometer fitted with a Metrohm combined glass electrode (model 6.0204.000) and a Hamilton Microlab M motor-driven syringe under the control of an appropriate program [27] running on an IBM PS/2 model 40 personal computer. The solution to be titrated was magnetically stirred and thermostatted at 298.2 ± 0.1 K in a water-jacketed vessel. A stream of water presaturated with nitrogen gas was passed over the solution in order to prevent contamination by atmospheric carbon dioxide. The electrode was calibrated in terms of hydrogen ion concentration $[H_3O^+]$ according to the Gran procedure [28] by titrating with 0.15 M NMe_4OH solution (about 0.7 cm^3) from the syringe known volumes (from 20 to 22 cm^3) of 0.015 M HCl solution, the ionic strength being adjusted to 0.15 M with NMe_4Cl. The log value of the ionic product of water ($K_w = [H_3O^+][OH^-]$) was found to be −13.80 under these conditions.

The potentiometric measurements were performed by adding the 0.15 M NMe_4OH solution to a solution containing $H_2Me_2DO2A\cdot 3HCl\cdot H_2O$ (*ca.* 1 mM). In the copper(II) complex formation experiments the solution in the vessel contained copper perchlorate and the ligand in approximately equimolar ratio. Owing to the known propensity of macrocyclic ligands containing carboxylate groups to form sodium complexes, potentiometric titrations have been made on solutions containing as inert electrolytes the two salts NMe_4Cl and $NaClO_4$ so adjusted that the total ionic strength was constant at 0.15 M. Such a procedure allowed us to determine the formation constant of a sodium complex formed with the ligand under investigation. Data were collected in the $-\log[H_3O^+]$ range 2.5–11.0; 157 data points from three curves were used for the determination of the protonation and sodium complex formation constants and 135 data points for the determination of the copper(II) complex formation constants. Equilibration of the titration solution following the addition of each aliquot of the hydroxide solution was attained fairly rapidly in the protonation experiments, whereas in the complex formation experiments it was necessary to wait up to 30 minutes to obtain a steady potential reading. The data were processed using the program HYPERQUAD.[29]

X-Band EPR spectra

X-Band EPR spectra were recorded on a Bruker Spectrometer ER 200-SR DD operating at $\nu = 9.44$ GHz. The H_0 applied external magnetic field was calibrated by using a Varian F-8 Fluxmeter and the operational frequency ν was tested with a Hewlett-Packard model X5-32B Wavemeter by using the solid state sample DPPH (stable diphenylpicrylhydrazyl free radical) as suitable field marker. The corresponding $g_{averaged}$ value was 2.0036. The actual temperature was controlled using a Bruker B-ST 100/70 unit with an accuracy of ±1 K. The a_i hyperfine splittings were measured by the peak-to-peak distance of the four copper(II) isotropic or anisotropic lines in both the correspondingly resolved signals, and the relevant A_i parameters calculated.[30] The isotropic EPR intensity I_{iso} measurements were obtained from the copper(II) isotropic spectra by using the relationship $I_{iso} = (\Delta H_{iso})^2 h$, where ΔH_{iso} is the linewidth of the $m_I = +3/2$ line (the fourth high-field copper(II) absorption line is the narrowest one) and h the corresponding height.[30] The best fit computed values of the copper(II) EPR parameters were evaluated by using appropriate simulation procedures (SIM14a and ESRMGR programs).[31] In order to have quantitative spectral reproducibility, the copper(II) complex samples were introduced into a calibrated quartz capillary tube permanently positioned in the rectangular resonance cavity.

Cyclic voltammetry

Cyclic voltammetry was performed in a three-electrode cell having a palladium disk working electrode (1.5 mm in diameter) surrounded by a platinum-spiral counter electrode and an aqueous saturated calomel reference electrode (SCE) mounted with a Luggin capillary. Either a BAS 100A electrochemical analyzer or a multipurpose Amel instrument (a Model 566 analog function generator and a model 522 potentiostat) were used as polarizing units. Controlled potential coulometry was performed in an H-shaped cell with anodic and cathodic compartments separated by a sintered-glass disk. The working macroelectrode was a platinum gauze; a mercury pool was used as the counter electrode. The Amel potentiostat was connected to an Amel Model 558 integrator. All the potential values are referred to the SCE.

Crystallography

Experimental data were recorded at room temperature on an Enraf-Nonius CAD4 diffractometer using graphite-monochromated Mo-Kα radiation. Atomic scattering factors were taken from ref. 32 with anomalous dispersion corrections from ref. 33. An empirical absorption correction was applied by using the program XABS [34] with transmission factors of 0.820 and 1.467. The computational work was performed with a Digital Dec 5000/200 workstation using SHELX 93 [35a] and SIR 92.[35b] The structure was solved by direct methods [36] and all non-hydrogen atoms were found through a series of F_o Fourier maps. Refinement was done by full-matrix least squares calculations, initially with isotropic thermal parameters, and then with anisotropic thermal parameters for all the atoms but the hydrogens. Crystallographic details are reported in Table 2.

CCDC reference number 186/2012.

See http://www.rsc.org/suppdata/dt/b0/b002441o/ for crystallographic files in .cif format.

Biodistribution studies

Rabbit was selected as animal model. The animal was anaesthetized and placed within the field of view (FOV) of the tomograph in the transaxial position (in this way the body of

Table 1 Comparison of the protonation constants for Me_2DO2A (298.2 K) with those of other related macrocycles

Ligand	log K_1	log K_2	log K_3	log K_4	Conditions
Me_2DO2A [a]	11.38(1)	10.38(1)	3.90(1)	2.30(1)	0.15 M NMe_4Cl
DO2A [b]	11.45(2)	9.45(3)	4.00(1)	2.36(3)	0.1 M NEt_4ClO_4
DO3A [c]	11.59(3)	9.24(3)	4.43(2)	3.48(3)	0.1 M NMe_4Cl
DOTA [c]	11.73(3)	9.40(2)	4.50(4)	4.19(6)	0.1 M NMe_4Cl
cyclen [d]	10.97	9.87	1.5	0.7	0.5 M KNO_3

Values in parentheses are standard deviations in the last significant figure. [a] This work. [b] Ref. 40. [c] Ref. 37; DO3A = 1,4,7,10-tetraazacyclododecane-1,4,7-triacetic acid, DOTA = 1,4,7,10-tetraazacyclododecane-1,4,7,10-tetraacetic acid. [d] Ref. 49.

the animal fitted exactly the dimensions of the PET scanner FOV and images spanned from head to tail). An aqueous solution (1 cm^3) of [$^{64}Cu(Me_2DO2A)$] (≈400 μCi), prepared as previously described, was diluted with saline (1 cm^3) and injected as a single bolus *via* the ear marginal vein of rabbit. Images were acquired by a CTI ECAT 911 4/12 PET scanner (4 rings of 512 BGO detectors; 4.5 cm axial field of view) having a transaxial spatial resolution of 6 mm. 15 frames of 1 min and 15 frames of 5 min starting at the moment of injection were acquired within a time of 90 min. Each frame yielded a set of 7 consecutive tomographic images (tomographic slice) each representing the topographic distribution of the radioactivity across the animal medial line (head to tail). Each tomographic slice was at about 4.5 mm from the other. The image unit (voxel = pixel dimensions × slice thickness) represented a volume of 70 μl.

Results and discussion

Synthesis and characterization of the macrocycle 4,10-dimethyl-1,4,7,10-tetraazacyclododecane-1,7-diacetic acid (H_2L)

This new macrocycle was synthesized by reaction of 1,7-dimethyl-1,4,7,10-tetraazacyclododecane with chloroacetic acid in alkaline solution at 70 °C for 15 h. Throughout the reaction time the pH value of the water solution was maintained in between 8.5 and 9.0 by addition of NaOH. The product separation was accomplished by ion-exchange chromatography. The ligand was isolated in its protonated form $H_2Me_2DO2A{\cdot}3HCl{\cdot}H_2O$ as a white solid which is soluble in both water and polar organic solvents (MeCN, $CHCl_3$).

The refined protonation constants of the conjugate base Me_2DO2A were determined by potentiometric titration of $H_2Me_2DO2A{\cdot}3HCl$ with NMe_4OH using 0.15 M NMe_4Cl as background electrolyte. The values obtained for K_1, K_2, K_3 and K_4 are reported in Table 1 and refer to the equations $L^{2-} + H^+ \rightleftharpoons HL^-$, $HL^- + H^+ \rightleftharpoons H_2L$, $H_2L + H^+ \rightleftharpoons H_3L^+$, $H_3L^+ + H^+ \rightleftharpoons H_4L^{2+}$, respectively. For comparative purposes, the protonation constants of some related macrocycles are given in Table 1. The pattern of the protonation constants is similar within the macrocycles examined [37] and consistent with the first two protonations occurring at two nitrogen atoms.

In line with all the other macrocycles, Me_2DO2A exhibits much larger constants for the first two protonations than for the third and fourth steps. For the parent macrocycle cyclen (1,4,7,10-tetraazacyclododecane), this trend is dramatically enhanced by the lack of carboxylate groups which makes the electrostatic repulsion within the highly protonated species H_3L^{3+} and H_4L^{4+} the factor responsible for the remarkable decrease of K_3 and K_4. Interestingly, the second protonation constant of Me_2DO2A is the highest among those reported for the macrocycles of Table 1. As compared to DO2A (1,4,7,10-tetraazacyclododecane-1,7-diacetic acid), this result apparently clashes with the general rule that tertiary amines are less basic than secondary amines in water. For macrocyclic polyamines, this phenomenon has previously been observed, however.[38]

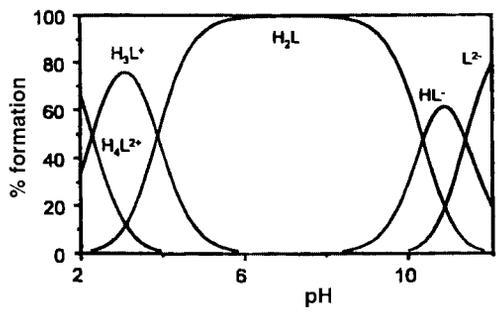

Fig. 1 Speciation diagram of Me_2DO2A protonation.

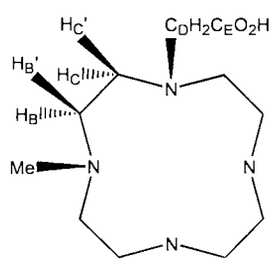

Fig. 2 Sketch of H_2Me_2DO2A with the labeling scheme used.

In the case of Me_2DO2A, one may argue whether the site of the first protonation is either a methyl-substituted N atom or an acetyl-substituted N atom. Notwithstanding that protonation of amines bearing a β-carboxylate group is often assisted by hydrogen bonding interaction with the acetate side-chain,[39] the first protonation of Me_2DO2A takes place at one of the methyl-substituted nitrogen atoms as shown by variable-pH ^1H and ^{13}C NMR titration experiments (see below). The second protonation similarly involves the *trans* NMe group, while the constants K_3 and K_4 are assigned to the protonations of the two carboxylate groups on the basis of ^{13}C NMR studies as well as the similar protonation pattern of DO2A.[40] The distribution of the chemical species derived from Me_2DO2A at different pH values is shown in Fig. 1.

In order to gain insight into the protonation process as well as the solution structure of the macrocycle, a ^1H and ^{13}C-{^1H} NMR analysis has been carried in the pH range from 1 to 13 using the potassium salt of the ligand. A sketch of the macrocyclic ligand together with the labeling scheme adopted for the NMR assignments is shown in Fig. 2. At very alkaline pH values (12.5, 25 °C), where, according to the potentiometric results, the only species in solution is the fully deprotonated dianion Me_2DO2A (L^{2-}), the macrocycle is fluxional as shown by three broad singlets of relative intensities 2:8:3 in the ^1H NMR spectrum (Fig. 3, trace g). These resonances are assigned to the acetate methylene protons (H_D), the ethylene bridge protons ($H_{BB'}/_{CC'}$) and the methyl protons (H_A). Independent of the pH value, the methylene (H_D) and methyl protons appear as two sharp singlets. On decreasing the pH, however, the ethylene bridge resonance gradually splits into four resolved signals of equal intensity ultimately to give a sharp ddd spin pattern at pH 2 (Fig. 3, trace a).

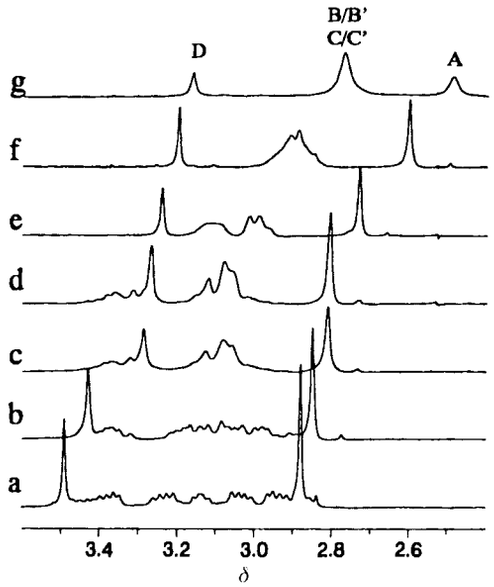

Fig. 3 ^{1}H NMR spectra of Me_2DO2A at different pH measured at 200 MHz and 25 °C: (a) pH 2; (b) 4; (c) 5; (d) 9; (e) 10.3; (f) 11; (g) 12.5.

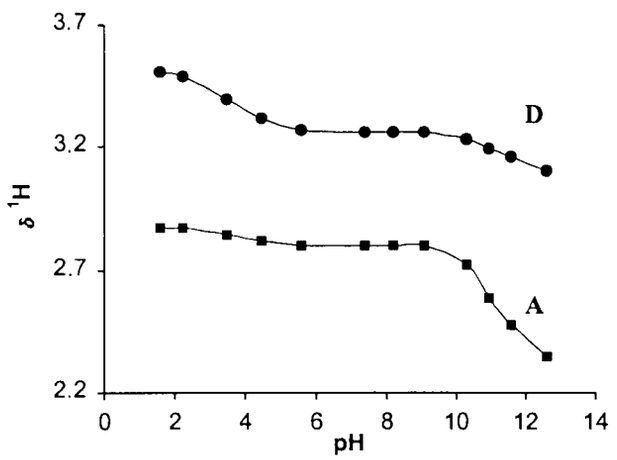

Fig. 4 ^{1}H NMR chemical shifts of H_A and H_D protons of Me_2DO2A *versus* pH measured at 200 MHz and 25 °C.

A plot of the chemical shifts observed for the methyl (H_A) and $CH_2CO_2^-$ (H_D) protons as a function of the pH value is shown in Fig. 4. From this, one may readily infer that the first strong inflection, between pH 12.5 and 9, involves proton H_A and, to a smaller extent, proton H_D. This finding is consistent with the potentiometric measurements and confirms that the first two protonations occur at the two nitrogen atoms bearing methyl groups. Indeed, it is known that the protonation of a basic site leads to a deshielding of the adjacent methyl groups and thus to a low-field shift of the corresponding resonance.[41] In accord with the potentiometric results, indicating that H_2L is the predominant species between pH 5 and 9, the ^{1}H NMR chemical shifts of the H_A and H_D nuclei do not significantly change in this pH range. The ^{1}H NMR spectrum recorded at pH 7 is shown in Fig. 5 (trace a, 20 °C; trace b, 90 °C). The assignments of the ^{1}H and ^{13}C resonances at pH 7 were obtained from 2-D ^{1}H COSY, ^{1}H–^{13}C correlations and ^{1}H NOESY spectra (reported as supplementary material). Variable-temperature ^{1}H NMR experiments showed that H_2L is not conformationally rigid over the temperature range from 4 to 90 °C. The ethylene chain protons give rise to four distinct signals at low temperature, whereas they collapse to two broad resonances of 1 : 1 relative intensity at higher temperature.

The ^{1}H NMR titration curve of Me_2DO2A (Fig. 4) shows a second strong inflection point at a pH value between 5 and 2 which is related to a significant shift of the acetate methylene

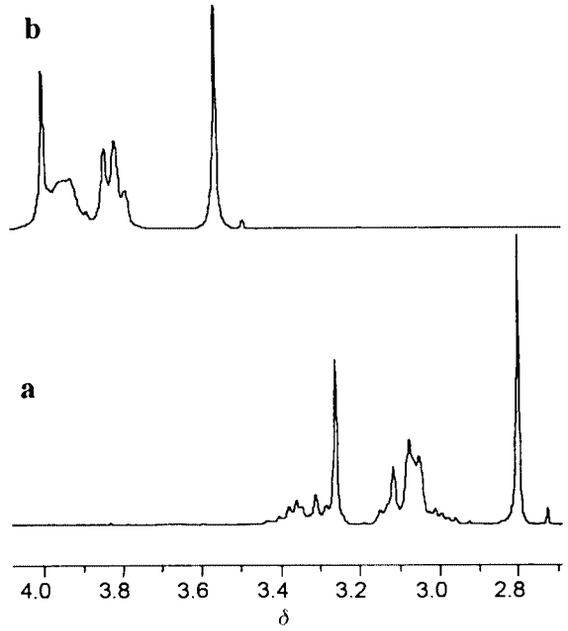

Fig. 5 ^{1}H NMR spectra of Me_2DO2A at pH 7: (a) at 20 °C; (b) at 90 °C.

protons (H_D). This effect is attributed to the occurrence of the third and fourth protonation steps at the carboxylate groups and ultimately supports the potentiometric results according to which the predominant species at pH 2 is the four-protonated dication H_4L^{2+}.

The H_4L^{2+} species has unambiguously been characterized in solution by means of ^{1}H and ^{13}C-{^{1}H} NMR spectroscopy. All the assignments were made on the basis of 2-D ^{1}H COSY, ^{1}H–^{13}C correlations and ^{1}H NOESY spectra. A section of the ^{1}H COSY and ^{1}H–^{13}C correlations together with the corresponding 1-D spectra is shown in Fig. 6. The ^{1}H NMR linewidth and the spin pattern do not change significantly in the temperature range from 4 to 70 °C, thus indicating that the dication is locked in a single preferred conformation on the NMR timescale.

A single set of ^{1}H and ^{13}C resonances for the A, B(B′), C(C′) and D nuclei are observed in the ^{1}H and ^{13}C-{^{1}H} spectra, thus showing that the four ethylene bridges as well as the two couples of CH_3N and CH_2CO_2 groups are chemically equivalent. The protons of each CH_2 bridging unit are diastereotopic with vicinal coupling constant $^3J_{HH}$ ($^3J_{CB} = 3.5$, $^3J_{C'B} = 7.2$, $^3J_{CB'} = 7.5$, $^3J_{C'B'} = 3.3$ Hz) consistent with a time-averaged preferred conformation close to that schematically represented in Fig. 7. A similar coupling pattern has been reported by Sherry and co-workers for the protons of the ethylene ring moiety in DO2A complexes with Mg^{II}, Ca^{II} and La^{III} at 75 °C.[42]

The conformation proposed in Fig. 7 is supported by the strong NOE interactions between the CH_3 and $H_{B'}$ protons and between the "CH_2CO_2" and $H_{B'}$ and $H_{C'}$ protons. The stereochemical rigidity of the tetraprotonated species H_4L^{2+} is attributed to the occurrence of both multiple hydrogen bonds within the macrocyclic ring and the presence of methyl-substituted nitrogen atoms. *trans* Couplings, as large as 14 Hz, which are typical for highly rigid macrocyclic rings, such as $La(DOTA)^{2-}$ described by Aime *et al.* have not been detected, however.[43]

A ^{13}C-{^{1}H} NMR study at different pH values has also been carried out. At pH 13, five peaks at δ 42.3 (C_A), 50.72 (C_C), 55.47 (C_B), 59.97 (C_D) and 181.8 (C_E) are observed. Decreasing the pH from 13 to 10 does not significantly affect these resonances which are only slightly shifted upfield. Below pH 5 the situation changes only for the C_E and C_D resonances that, at pH 1, move from δ 180.24 and 58.5 to 176.4 and 55.04, respectively, thus indicating that the third and fourth protonations take place at the carboxylate groups. The ^{13}C-{^{1}H}

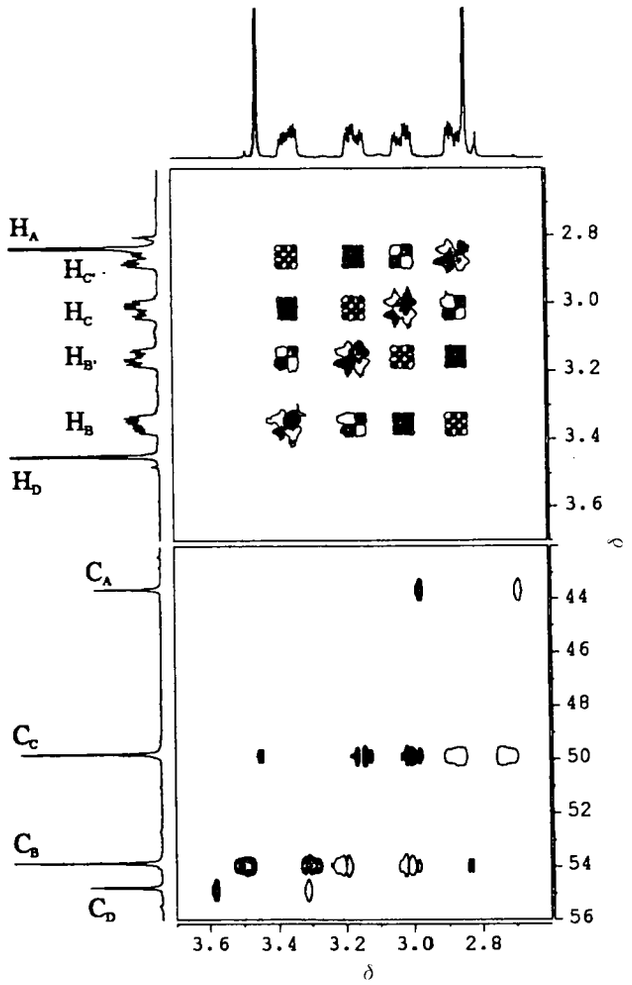

Fig. 6 Section of a 2-D ^{1}H COSY NMR spectrum (upper) and ^{1}H–^{13}C NMR correlations (lower) of the species H_4L^{2+} (D_2O, pH 2, 25 °C). Filled and empty circles represent positively and negatively phased peaks, respectively.

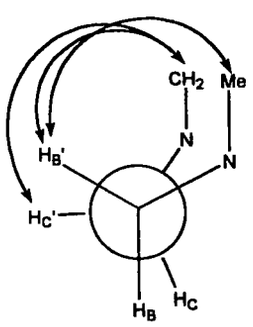

Fig. 7 Schematic representation of the conformation of each $CH_3NCH_2CH_2NCH_2CO_2$ unit in the dication H_4L^{2+}. Significant NOE interactions are indicated by arrows (500.132 MHz, 25 °C, mixing time 600 ms).

NMR spectrum of $H_2Me_2DO2A{\cdot}3HCl$ in D_2O contains five sharp peaks at δ 43.59 (C_A), 49.8 (C_C), 53.85 (C_B), 54.78 (C_D) and 176.09 (C_E).

Synthesis and characterization of [Cu(Me$_2$DO2A)]

The reaction of hydrated $Cu(ClO_4)_2$ with an aqueous solution of $H_2Me_2DO2A{\cdot}3HCl$ at pH 7.4 yields a neutral blue complex which analyzes as $[Cu(Me_2DO2A)]{\cdot}3H_2O$. The complex is soluble in water and in MeOH but not in BuOH. In the IR spectrum, the $\nu_{asym}(CO_2^-)$ band falls at 1610 cm^{-1} as expected for η^1-O acetate groups.[44]

The solid state structure of $[Cu(Me_2DO2A)]{\cdot}3H_2O$ has been determined by a single crystal X-ray diffraction analysis. In

Table 2 Summary of crystallographic data for the complex [Cu(Me$_2$-DO2A)]·3H$_2$O

Chemical formula	$C_{14}H_{26}CuN_4O_4$
Formula weight	377.93
Crystal system	Orthorhombic
Space group	*Fdd*2
μ/mm^{-1}	1.378
a/Å	24.419(5)
b/Å	31.207(5)
c/Å	8.475(5)
V/Å^3	6458(4)
T/K	293(2)
Z	16
Measured/independent reflections	1962 [*R*(int) = 0.0000]
Final *R*1, *wR*2 [$I > 2\sigma(I)$] (all data)	0.0318, 0.0835 0.0372, 0.0864

Table 3 Selected bond lengths [Å] and angles [°]

Cu(1)–O(2)	1.952(3)	Cu(1)–N(4)	2.143(3)
Cu(1)–O(1)	1.985(3)	Cu(1)–N(3)	2.303(3)
Cu(1)–N(2)	2.101(3)	Cu(1)–N(1)	2.322(4)
O(2)–Cu(1)–O(1)	89.29(12)	N(2)–Cu(1)–N(3)	80.26(14)
O(2)–Cu(1)–N(2)	171.96(12)	N(4)–Cu(1)–N(3)	81.72(12)
O(1)–Cu(1)–N(2)	83.75(12)	O(2)–Cu(1)–N(1)	102.13(13)
O(2)–Cu(1)–N(4)	83.96(11)	O(1)–Cu(1)–N(1)	92.01(13)
O(1)–Cu(1)–N(4)	168.55(12)	N(2)–Cu(1)–N(1)	82.21(13)
N(2)–Cu(1)–N(4)	103.55(11)	N(4)–Cu(1)–N(1)	80.43(12)
O(2)–Cu(1)–N(3)	98.21(13)	N(3)–Cu(1)–N(1)	151.23(12)
O(1)–Cu(1)–N(3)	108.47(12)		

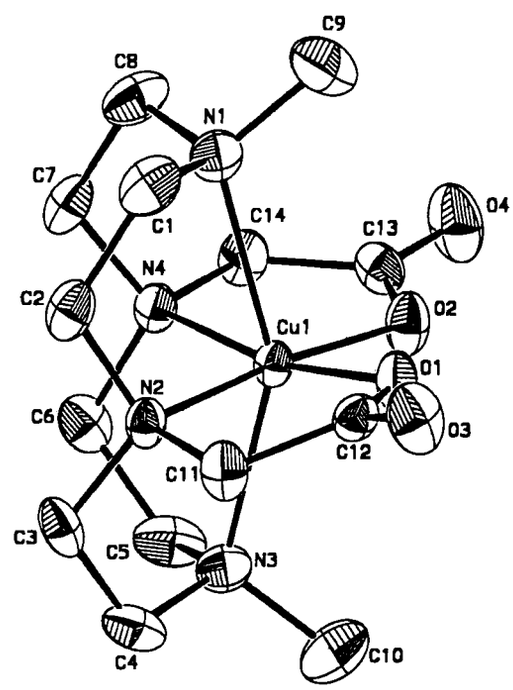

Fig. 8 A ZORTEP drawing of the [Cu(Me$_2$DO2A)] complex.

Fig. 8 is reported a ZORTEP[45] drawing of the molecular structure with the atomic labeling scheme; selected bond lengths and angles are given in Table 3. The structure consists of mononuclear molecules in which each copper(II) ion lies at the center of a distorted octahedron. The macrocyclic ligand coordinates the metal ion through its four tertiary amine groups in a folded manner as shown by the equatorial N(2)–Cu(1)–N(4) angle and the axial N(1)–Cu(1)–N(3) angle of 103.55(11) and 151.23(12)° respectively. Such a folding is typical for similar polyazamacrocycles.[23,40] The four Cu–N bonds are significantly different from each other. The axial nitrogen atoms N(1) and

Table 4 Thermodynamic stability constants at 298 K for Me_2DO2A with copper(II) and sodium ions. $I = 0.15$ M NMe_4Cl

Reaction	
$Cu^{2+} + L^{2-} \rightleftharpoons CuL$	20.85(3)
$Cu^{2+} + HL^{-} \rightleftharpoons Cu(HL)^{+}$	12.74(4)
$CuL + H^{+} \rightleftharpoons Cu(HL)^{+}$	3.27(4)
$Na^{+} + L^{2-} \rightleftharpoons NaL^{-}$	1.96(1)

Values in parentheses are standard deviations on the last significant figure.

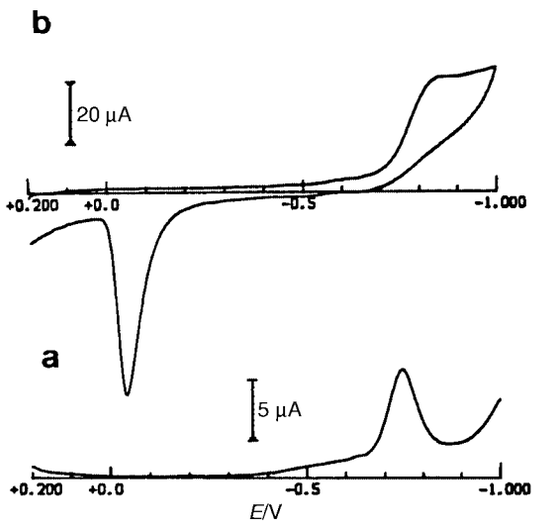

Fig. 9 Cyclic (a) and differential pulse (b) voltammograms recorded at a platinum electrode on an aqueous (phosphate buffer, pH 7.4) solution of $[Cu(Me_2DO2A)]$ (2.0×10^{-3} M). Scan rates: (a) 0.2; (b) 0.004 V s^{-1}.

N(3) exhibit much longer Cu–N bonds than the equatorial ones N(2) and N(4), probably due to steric reasons. The methyl groups bonded to the axial nitrogen atoms N(1) and N(3) exhibit a *cis* configuration with respect to the idealized macrocyclic plane. Two *cis* carboxylic groups complete the metal coordination in the equatorial plane using the oxygen atoms O(1) and O(2), respectively. The two co-ordinated oxygen atoms deviate from the equatorial plane defined by N(2), Cu(1), N(4) by 0.307(0.005) and −0.100(0.005) Å, respectively.

The stability of $[Cu(Me_2DO2A)]$ in water solution has been determined by potentiometric titration. The thermodynamic stability constants for the formation of the copper(II) complex are reported in Table 4 which also contains data for the formation of the Na^+ adduct. The ligand Me_2DO2A forms two highly stable copper(II) complexes in which the macrocycle behaves as either a pentadentate ($CuHL^+$) or hexadentate ligand (CuL). At pH 7.4 the potentiometric measurements show the exclusive formation of CuL.

The electrochemical stability of $[Cu(Me_2DO2A)]$ in water has also been evaluated by electrochemical measurements. Fig. 9 shows the voltammetric behavior in buffered (pH 7.4) aqueous solution of the complex in either cyclic or differential pulse voltammetry. The complex undergoes an irreversible reduction, which, as shown by the appearance of the anodic stripping peak in the cyclic voltammetric backscan illustrated in Fig. 9(a), involves an overall two-electron step accompanied by decomplexation and subsequent electrodeposition of copper metal. No trace of any directly associated reoxidation process was detected even at the scan rate of 1 V s^{-1}. The concomitance of two one-electron steps is confirmed by the fact that no resolution is gained in differential pulse voltammetry (Fig. 9b).

The absence of reversible Cu^{II}–Cu^{I} reduction suggests that the ligand assembly is not sufficiently flexible to support the increase of the ionic radius, thus leading to framework destruction. Finally, the rather negative value of the reduction process ($E_p = -0.81$ V, *vs.* SCE, at 0.2 V s^{-1}) testifies to the stability of the copper(II) assembly.

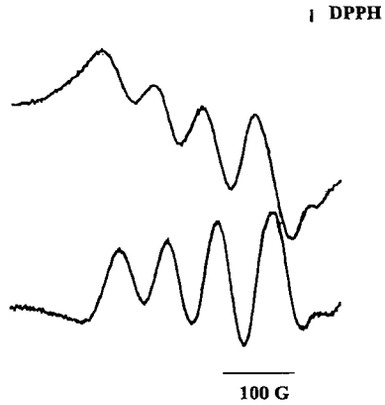

Fig. 10 X-Band EPR spectra of $[Cu(Me_2DO2A)]$ in aqueous solution at pH 7.4 (298 K).

The paramagnetic character does not allow one straightforwardly to determine the solution structure of $[Cu(Me_2DO2A)]\cdot 3H_2O$ by NMR spectroscopy. For this reason, an EPR study was carried out. Fig. 10 shows the X-band EPR spectrum of the complex in water at pH 7.4. The relevant magnetic parameters are collected in Table 5. The fluid solution signal at room temperature is relatively broad with partial resolution of the copper(II) isotropic hyperfine (hpf) structure with $g_{iso} > g_{electron} = 2.0023$ (^{63}Cu, natural abundance = 69.09%; ^{65}Cu, natural abundance = 30.91%; $I_{Cu\text{-}63} = I_{Cu\text{-}65} = 3/2$). The spectrum exhibits a significant ΔH_{iso} linewidth variation depending on the four copper m_I values. The EPR features are consistent with a noticeable "$3d^9$" orbital contribution to the SOMO and are indicative of a significant value of the corresponding λ spin–orbit coupling constant (>0). They also indicate the presence of structural anisotropies affecting the co-ordination sphere which are not completely averaged under the fluid solution fast motion conditions.[30] No nitrogen superhyperfine (shpf) resolution is evident in the fourth narrowest line ($m_I = +3/2$) even in the second derivative mode, due to the actual ΔH_{iso} largely overlapping the corresponding N ligands shpf splittings (if any). Assuming a distorted octahedral co-ordination, an upper value of $\Delta H_{iso}(m_I = +3/2) = 5.1 \times 10^{-3}$ $cm^{-1} \geq A_{iso}(N)$ may be calculated for the relevant isotropic shpf interaction. The isotropic spectral intensity I accounts for the quantitative presence of $[Cu(Me_2DO2A)]$.

In the glassy state ($T = 100$ K) the EPR parameters are typical of a well resolved copper(II) axial structure with $g_\parallel > g_\perp > g_{electron}$ and $A_\parallel > A_\perp$. The relevant $\langle g \rangle$ and $\langle A \rangle$ averaged parameters [$\langle g \rangle = \frac{1}{3}(g_\parallel + 2g_\perp)$, $\langle A \rangle = \frac{1}{3}(A_\parallel + 2A_\perp)$] are in good agreement with the corresponding isotropic ones, suggesting that even under different experimental conditions the main copper(II) complexation geometry is basically retained.

The room-temperature X-band EPR spectrum of solid $[Cu(Me_2DO2A)]$ consists of a very broad, axial lineshape ($g_\parallel > g_\perp > g_{electron}$) with an overall ΔH of 185.0(8) G. At 100 K the signal is still unresolved. The spectral features are typical of strong spin–spin magnetic interactions occurring in the microcrystalline copper(II) powder, so that the $g_\parallel$ and $g_\perp$ regions nearly collapse in a broad signal without any A_{aniso} spectral resolution.

On the basis of the Blumberg–Peisach approach, which accounts for the close relationship between $g_\parallel$ and $A_\parallel$ for equatorially co-ordinated $S = \frac{1}{2}$ paramagnetic metal complexes (in both glassy solution and the solid state), some important properties of copper(II) compounds may be determined.[46–48] In the case at hand, the actual composition of the equatorial atom donor set and the concomitant electric charge may be evaluated from the glassy solution EPR spectrum. The tetrahedral

Table 5 X-Band EPR parameters of the [Cu(Me_2DO2A)] complex in aqueous solution (RT and liquid nitrogen) and the solid state, respectively

$g_\parallel$	$g_\perp$	$\langle g\rangle^a$	g_{iso}	$A_\parallel{}^b$	$A_\perp{}^b$	$\langle A\rangle^{a,b}$	$A_{iso}{}^b$	$A(N)^{b,c}$
2.250	2.062(5)	2.125(5)	2.116(5)	15.8(6)	≤3.5(6)	≤7.7(6)	7.8(6)	≤5.1/8(6)
2.119(8)[d]				≤18.4(8)[d]	≤18.4(8)[d]			

[a] $\langle g\rangle = \frac{1}{3}(g_\parallel + 2g_\perp)$, $\langle A\rangle = \frac{1}{3}(A_\parallel + 2A_\perp)$. [b] A_i in 10^{-3} cm^{-1}. [c] Nitrogen isotropic shpf coupling constant value. [d] g_i and A_i solid state anisotropic averaged values.

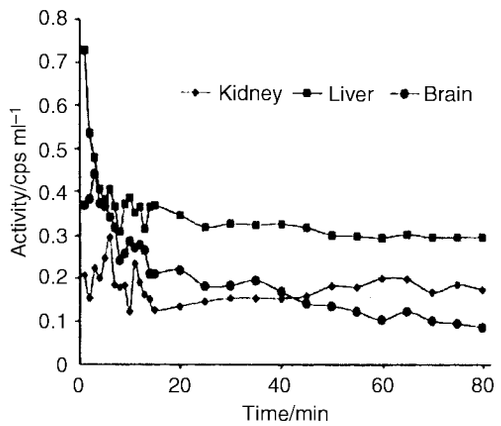

Fig. 11 Biodistribution of [^{64}Cu(Me_2DO2A)] in kidney, liver and brain of rabbit as determined by PET.

distortion parameter $f = g_\parallel/A_\parallel$ for an aqueous solution of [Cu(Me_2DO2A)] is 0.144 cm which, according to the Blumberg–Peisach theory for octahedral copper(II) complexes,[46] lies on the borderline between N_2O_2 and N_3O donor atom sets with an equatorial charge of 0 and +1, respectively. The solid state structure of [Cu(Me_2DO2A)] as determined by the X-ray analysis shows a distorted octahedral geometry in which the equatorial plane is best defined by two nitrogen and two oxygen atoms. In water solution, hydrogen bonding interactions involving the carboxylate groups may lengthen the Cu–O bonds and ultimately result in a further distortion of the octahedral geometry.

Biodistribution studies

A preliminary biodistribution evaluation has shown that early images of [^{64}Cu(Me_2DO2A)] reflect body vascularization then the radiotracer reaches quite quickly the emunctory organs: liver first then kidneys and bladder. Kinetic data for liver, kidney and brain are reported in Fig. 11 and shown as a plot of radioactivity concentration (counts per second cm^{-3}) *versus* elapsed time from injection. The highest radioactivity is accumulated by the liver; this value decreases in the first 10 min as a consequence of the first pass of the bolus of radioactivity, then remains constant for the entire time, showing a slow clearance. Activity in kidney shows a similar behavior.

Uptake in the brain is quite low but was significant. This last result is very important because activity in brain, even if low, indicates that [^{64}Cu(Me_2DO2A)] is able to cross the blood–brain barrier, in accordance with the hypothesis of the neutral charge of the present copper-64 complex. Delayed images have not been obtained with this animal model due to the PET sensitivity limit related to the reduction in count rate for radiotracer decay and organ washout.

Concluding remarks

A new tetraazamacrocycle bearing two *trans* carboxylic arms has been synthesized and fully characterized. It has been found to react with copper(II) salts in aqueous solution to give the neutral octahedral complex [Cu(Me_2DO2A)] which has been characterized in both the solid state and solution. The use of $^{64}CuCl_2$ as metal source has provided the radioactive derivative [^{64}Cu(Me_2DO2A)]. Though preliminary results concerning the use of [^{64}Cu(Me_2DO2A)] in nuclear medicine are at an early stage of development, the information obtained is quite promising and suggests one should continue the study of this kind of radiotracers through the development of different ligand structures as well as methods of generating ^{64}Cu salts. Indeed, unlike related ^{64}Cu-labeled macrocyclic complexes,[22] [^{64}Cu(Me_2DO2A)] has also been found to cross the blood–brain barrier.

Acknowledgements

Regione Toscana (RRAT) is gratefully acknowledged for financial support. Thanks are due to Professor Piero Zanello (University of Siena, Italy) for assistance in the electrochemical study, Mr Oreste Sorace (IFC-CNR) for carrying out the PET acquisitions, Mr Luigi Taddei (IFC-CNR) for assistance with animal experiments and to Dr W. Oberhauser (ISSECC-CNR) for helpful discussion.

References

1 K. P. Wainwright, *Coord. Chem. Rev.*, 1997, **166**, 35; J. Chapman, G. Ferguson, J. F. Gallagher, M. C. Jennings and D. Parker, *J. Chem. Soc.*, *Dalton Trans.*, 1992, 345; L. F. Lindoy, *The Chemistry of Macrocyclic Ligand Complexes*, Cambridge University Press, Cambridge, 1989; R. D. Hancock and A. E. Martell, *Chem. Rev.*, 1989, **89**, 1875; P. V. Bernhardt and G. A. Lawrance, *Coord. Chem. Rev.*, 1990, **104**, 297; D. Parker, K. Pulukkody, T. J. Normann, A. Harrison, L. Royle and C. Walker, *J. Chem. Soc.*, *Chem. Commun.*, 1992, 1441; R. Dhillon, A. K. W. Stephens, S. L. Whitbread, S. F. Lincoln and K. P. Wainwright, *J. Chem. Soc.*, *Chem. Commun.*, 1995, 97; H. Maumela, R. D. Hancock, L. Carlton, J. H. Reibenspies and K. P. Wainwright, *J. Am. Chem. Soc.*, 1995, **117**, 6698; M. G. B. Drew, *Coord. Chem. Rev.*, 1977, **24**, 179; M. Spirlet, J. Rebizant and J. F. Desreux, *Inorg. Chem.*, 1984, **23**, 359; I. Murase, I. Ueda, N. Marubayashi, S. Kida, N. Matsumoto, M. Kudo, M. Toyohara, K. Hiate and M. Mikuriya, *J. Chem. Soc.*, *Dalton Trans.*, 1990, 2763; L. H. Tan, M. R. Taylor, K. P. Wainwright and P. A. Duckworth, *J. Chem. Soc.*, *Dalton Trans.*, 1993, 2921; M. Di Varia, F. Mani, N. Nardi, P. Stoppioni and A. Vacca, *J. Chem. Soc.*, *Dalton Trans.*, 1996, 2679.

2 C. J. Anderson and M. J. Welch, *Chem. Rev.*, 1999, **99**, 2219; S. Liu and D. S. Edwards, *Chem. Rev.*, 1999, **99**, 2235; E. Soini, L. Hemmila and P. Dhalen, *Ann. Biol. Clin.* (*Paris*), 1990, **48**, 567; R. A. Evangalista, A. Pollak, B. Allore, E. F. Templeton, R. C. Morton and E. P. Diamandis, *Clin. Biochem.*, 1988, **21**, 173; E. Lopez, C. Chypre, B. Alpha and G. Mathis, *Clin. Chem.*, 1993, **39**, 196; G. Mathis, *Clin. Chem.*, 1995, **41**, 1391; E. Soini and H. Kojola, *Clin. Chem.*, 1983, **29**, 65; I. Hemmila, V. M. Mukkala and S. Dakubu, *Anal. Biochem.*, 1984, **137**, 375; E. F. G. Dickson, A. Pollak and E. P. Diamandis, *Photochem. Photobiol.*, 1995, **27**, 3; A. D. Sherry, *J. Less-Common Met.*, 1989, **149**, 133; D. Parker, *Chem. Br.*, 1994, 893; *Comprehensive Supramolecular Chemistry*, eds. J. M. Lehn, D. D. Macnicol, J. L. Atwood, J. E. Davies, D. N. Reinhoudt and F. Vogtle, Pergamon, Oxford, 1996, vol. 1, ch. 17; S. Aime, M. Botta and E. Terreno, *Chem. Soc. Rev.*, 1998, **27**, 19.

3 W. A. Volker and T. J. Hoffmann, *Chem. Rev.*, 1999, **99**, 2269; V. Alexander, *Chem. Rev.*, 1995, **95**, 273; D. Parker, *Chem. Soc. Rev.*, 1990, **19**, 271; D. Parker and K. J. Jankowski, in *Advances in Metals in Medicine*, eds. M. J. Abrams and B. A. Murrer, Jai Press, New York, 1993, vol. 1, ch. 2, p. 29; K. Devreese, V. Kofler-Mongold, C. Leutgeb, V. Weber, K. Vermeire, S. Schacht, J. Anne, E. De Clercq, R. Datema and G. Werner, *J. Virol.*, 1996, **70**, 689.

4 M. K. Moi, C. F. Meares, M. J. McCall, W. C. Cole and S. J. DeNardo, *Anal. Biochem.*, 1985, **148**, 249.

5 J. F. Desreux, *Inorg. Chem.*, 1980, **19**, 1319; X. Wang, T. Jin, V. Comblin, A. Lopez-Mut, E. Merciny and F. Desreux, *Inorg. Chem.*, 1992, **31**, 1095; S. Aime, A. S. Batsanov, M. Botta, J. A. K. Howard, D. Parker, K. Senanayake and G. Williams, *Inorg. Chem.*, 1994, **33**, 4696; C. J. Broan, K. J. Jankovski, R. Kataki, D. Parker, A. Randall and A. Harrison, *J. Chem. Soc.*, *Chem. Commun.*, 1990, 1739.

6 J. R. Morrow, S. Amin, C. H. Lake and M. R. Churchill, *Inorg. Chem.*, 1993, **32**, 4566; L. Carlton, R. D. Hancock, H. Maumela and K. P. Wainwright, *J. Chem. Soc.*, *Chem. Commun.*, 1994, 1007; S. Aime, A. Barge, M. Botta, D. Parker and A. S. De Sousa, *J. Am. Chem. Soc.*, 1997, **119**, 4767; P. Pittet, G. S. Laurence, S. F. Lincoln, M. L. Turonet and K. P. Wainwright, *J. Chem. Soc.*, *Chem. Commun.*, 1991, 1205; A. K. W. Stephens and S. F. Lincoln, *J. Chem. Soc.*, *Dalton Trans.*, 1993, 2123.

7 P. J. Blower, J. S. Lewis and J. Zweit, *Nucl. Med. Biol.*, 1996, **23**, 957.

8 C. J. Anderson, J. M. Connett, S. W. Schwarz, P. A. Rocque, L. W. Guo, G. W. Philpott, K. R. Zinn, C. F. Meares and M. J. Welk, *J. Nucl. Med.*, 1992, **33**, 1685.

9 B. E. Rogers, C. J. Anderson, J. M. Connett, L. W. Guo, W. B. Edwards and E. L. C. Sherman, *Bioconjugate Chem.*, 1996, **7**, 511.

10 P. M. Smith-Jones, R. Fridich, T. A. Kaden, I. Novak-Hofer, K. Siebold, D. Tschudin and H. R. Maecke, *Bioconjugate Chem.*, 1991, **2**, 415.

11 C. J. Anderson, P A. Rocque, P. A. Weinheimer, J. Mathias and M. J. Welch, *J. Nucl. Med.*, 1993, **34**, 461; J. Mathias, M. J. Welch, M. A. Gren, H. Diril, C. F. Meares, R. J. Gropler and S. R. Bergmann, *J. Nucl. Med.*, 1990, **32**, 475.

12 O. D. M. Hughes, M. C. Bishop, A. C. Perhins, M. Frier, M. R. Price and G. Denton, *E. J. Nucl. Med.*, 1997, **24**, 439.

13 D. L. Kukis, H. Diril, D. P. Greiner, S. J. DeNardo, G. L. DeNardo, Q. A. Salaco and C. F. Meares, *Cancer*, 1994, **73**, 779.

14 I. Novak-Hofer, H. P. Amstutz, H. R. Macke, R. Schwarzbach, K. Zimmermann, J. J. Morgenthaler and P. A. Schubiger, *Cancer Res.*, 1995, **55**, 46.

15 G. L. DeNardo and S. J. DeNardo, in *Cancer Therapy with Radiolabeled Antibody*, ed. D. M. Goldenberg, CRC Press, Inc., Boca Raton, FL, 1995, p. 217.

16 C. J. Anderson, S. W. Schwarz, J. M. Connett, P. D. Cutler, L. W. Guo, G. J. Germain, G. W. Philpott, K. R. Zinn, D. P. Greiner, C. F. Meares and M. J. Welch, *J. Nucl. Med.*, 1995, **36**, 850.

17 B. E. Rogers, C. J. Anderson, J. M. Connett, L. W. Guo, K. R. Zinn and M. J. Welch. *J. Labelled Compd. Radiopharm.*, 1995, **37**, 544.

18 C. J. Anderson, B. E. Rogers, J. M. Connett, L. W. Guo, K. R. Zinn, S. W. Schwarz and M. J. Welch, *J. Labelled Compd. Radiopharm.*, 1994, **35**, 313.

19 G. W. Philpott, S. W. Schwarz, C. J. Anderson, F. Dehdashti, J. M. Connett, K. R. Zinn, C. F. Meares, P. D. Cutler, M. J. Welk and B. A. Siegel, *J. Nucl. Med.*, 1995, **36**, 1818.

20 K. L. Kolsky, V. Joshi, G. E. Meinken, M. Sweet, L. F. Mausner and S. C. Srivastava, *J. Nucl. Med.*, 1994, **35**, 259P.

21 R. C. Mease, M. Chinol, L. F. Mausner, Z. Steplewski and S. C. Srivastava, *J. Nucl. Med.*, 1992, **35**, 942P.

22 T. M. Jones-Wilson, K. D. Deal, C. J. Anderson, D. W. McCarthy, Z. Kovacs, R. J. Motekaitis, A. D. Sherry, A. E. Martell and M. J. Welch, *Nucl. Med. Biol.*, 1998, **25**, 523.

23 M. Ciampolini, M. Micheloni, N. Nardi, P. Paoletti, P. Dapporto and F. Zanobini, *J. Chem. Soc.*, *Dalton Trans.*, 1984, 1357.

24 M. F. Summers, L. G. Marzilli and A. Bax, *J. Am. Chem. Soc.*, 1986, **108**, 4285.

25 V. Sklener, H. Miyashiro, G. Zon, H. T. Miles and A. Bax, *FEBS Lett.*, 1986, **208**, 94.

26 (*a*) P. K. Glasoe and F. A. Long, *J. Phys. Chem.*, 1960, **64**, 188; (*b*) K. Mikkelsen and S. O. Nielsen, *J. Phys. Chem.*, 1960, **64**, 632; (*c*) R. G. Bates, *Determination of pH. Theory and Practice*, Wiley, New York, 2nd edn., 1973, pp. 252, 253 and 375, 376; (*d*) R. Delgado, J. J Frausto Da Silva, M. T. S. Amorim, M. F. Cabral, S. Chaves and S. Costa, *Anal. Chim. Acta*, 1991, **245**, 271.

27 M. Fontanelli and M. Micheloni, *Proceedings of the 1st Spanish–Italian Congress on Thermodynamics of Complexes*, *Peniscola*, *Spain*, 3–6th June 1990.

28 G. Gran, *Analyst* (*London*), 1952, **77**, 661.

29 P. Gans, A. Sabatini and A. Vacca, *J. Chem. Soc.*, *Dalton Trans.*, 1985, 1195.

30 F. E. Mabbs and D. Collison, in *Electron Paramagnetic Resonance of d Transition Metal Compounds*, Elsevier, New York, 1992.

31 P. Lozos, B. M. Hoffman and C. G. Franz, Quantum Chemistry Program Exchange, Indiana University, 1974, vol. 20, p. 295.

32 A. J. C. Wilson (Editor), *International Tables for X-Ray Crystallography*, Kluwer Academic Publisher, Dordrecht, 1992, vol. C, p. 500.

33 A. J. C. Wilson (Editor), *International Tables for X-Ray Crystallography*, Kluwer Academic Publisher, Dordrecht, 1992, vol. C, p. 219.

34 S. Parkin, B. Moezzi and H. Hope, *J. Appl. Crystallogr.*, 1995, **28**, 53.

35 (*a*) G. M. Sheldrick, SHELX 93, University of Göttingen, 1993; (*b*) A. Altomare, G. Cascarano, C. Giacovazzo and A. Guagliardi, *J. Appl. Crystallogr.*, 1993, **26**, 343.

36 A. Altomare, G. Cascarano, C. Giacovazzo, A. Guagliardi, M. C. Burla and G. M. Polidori, *J. Appl. Crystallogr.*, 1994, **27**, 435.

37 K. Kumar, C. A. Chang, L. C. Francesconi, D. D. Dischino, M. F. Malley, J. Z. Gougoutas and M. F. Tweedle, *Inorg. Chem.*, 1994, **33**, 3567.

38 C. F. G. C. Geraldes, M. C. Alpoine, M. P. M. Marques, A. D. Sherry and M. Singh, *Inorg. Chem.*, 1985, **24**, 3876; A. Bianchi, M. Micheloni and P. Paoletti, *Coord. Chem. Rev.*, 1991, **110**, 17.

39 C. F. G. C. Geraldes, A. D. Sherry, M. P. M. Marques, M. C. Alpoine and S. Cortes, *J. Chem. Soc.*, *Perkin Trans.*, 1991, **2**, 137.

40 J. M. Weeks, M. R. Taylor and K. P. Wainwright, *J. Chem. Soc.*, *Dalton Trans.*, 1997, 317.

41 F. Desreux, E. Merciny and M. F. Leoncin, *Inorg. Chem.*, 1981, **20**, 987.

42 J. Huskens, D. A. Torres, Z. Kovacs, J. P. Andrè, C. F. G. Geraldes and A. D. Sherry, *Inorg. Chem.*, 1997, **36**, 312.

43 S. Aime, M. Botta, F. Fedelli and F. Uggeri, *Inorg. Chem.*, 1992, **31**, 2422.

44 M. Di Varia, F. Mani and P. Stoppioni, *J. Chem. Soc.*, *Dalton Trans.*, 1998, 1879.

45 L. Zsolmai and H. Pzitzkow, ORTEP original program modified for PC, University of Heidelberg, Germany, 1994.

46 J. Peisach and W. E. Blumberg, *Arch. Biochem. Biophys.*, 1974, **175**, 691.

47 N. D. Chasteen, in *Vanadium in Biological System. Physiology and Biochemistry*, Kluwer Academic Publisher, Dordrecht, 1990.

48 M. Casolaro, M. Chelli, M. Ginanneschi, F. Laschi, M. Muiz-Miranda, A. M. Papini and G. Sbrana, *Spectrochim. Acta*, 1999, **55**, 1675.

49 M. Kodama and E. Kimura, *J. Chem. Soc.*, *Chem. Commun.*, 1975, 326.